forests

MDPI

Article

A Novel Laser-Based Tree-Pulling Test Method to Measure Stem Inclination, Bending, and Spatially Resolved Structural Stiffness

Steffen Rust [1,*], Lothar Göcke [2], Josefine Liebisch [1], Ana Paula Coelho-Duarte [3], Agustina Sergio [3], Andreas Detter [4] and Bernhard Stoinski [5]

[1] Faculty of Resource Management, University of Applied Sciences and Arts, Büsgenweg 1a, 37077 Göttingen, Germany; j.liebisch@posteo.de
[2] Schwaaner-Landstr. 35E, 18059 Rostock, Germany; lothar@tree-inspection-technologies.de
[3] Forestry Department, Faculty of Agronomy, Universidad de la República, Montevideo 12900, Uruguay; paula.coelho@fagro.edu.uy (A.P.C.-D.); magustinasergio@gmail.com (A.S.)
[4] Brudi & Partner TreeConsult, Berengariastr. 9, 82131 Gauting, Germany; a.detter@tree-consult.org
[5] Private Institute for Dynamic Logic, Herforder Straße 15, 50737 Köln, Germany; bernhard.stoinski@pifdl.eu
* Correspondence: steffen.rust@hawk.de

Abstract

Tree mechanical stability is essential for forest management and urban safety. Although static pulling tests are currently the standard for non-destructive advanced risk assessments, these tests have significant methodological limitations. Large trees require high applied forces to produce measurable signals, which poses safety risks and causes equipment wear. Conversely, structurally compromised ancient, veteran, or dead trees (snags) may yield poor signal-to-noise ratios at low loads, leading to unstable model fits and unreliable safety factor extrapolations. Additionally, standard inclinometers often experience interference from motion-induced accelerations. This study introduces a high-resolution, low-noise measurement approach that resolves small basal inclinations and stem bending responses. This method uses laser-based tracking to monitor stem bending, torsion, and inclination under mechanical load. Experimental data were collected by combining traditional pulling tests with this novel system, as well as by conducting a pilot study that monitored tree movement during low-strength wind gusts. The proposed method enables more precise characterization of the initial load-response curve. Improving the signal-to-noise ratio at lower force levels allows for more robust safety extrapolations. When combined with a 3D LiDAR scan, the method can reveal deviations from the theoretical bending line in order to locate internal defects and variations in wood properties. These findings bridge a critical gap in tree risk assessment by improving the applicability of static testing to massive trees, as well as ecologically valuable yet structurally vulnerable snags and ancient and veteran trees.

Keywords: tree risk assessment; Static Load Test; non-destructive testing; standing deadwood; snag assessment; dynamic wind response; laser-based deflectometer

Received: 24 March 2026
Revised: 16 April 2026
Accepted: 23 April 2026
Published: 27 April 2026

1. Introduction

The mechanical stability of trees is essential for forest management, urban safety, and ecological resilience. Trees are frequently exposed to mechanical loads, particularly wind, which can cause stem bending and root plate inclination, potentially leading to stem fracture or uprooting [1–3]. Such failures, although of ecological importance [4,5], can result

in significant ecological and economic damage and may lead to personal injury, especially in urban and managed forest environments [1,6].

Although the risk of tree failure is generally low, a study in the Netherlands reported a rise in the standardized rate of injuries caused by tree failure in urban areas, increasing from 0.14 to 0.91 per 1,000,000 population between 1998 and 2021—an annual increase of 3% [7]. This trend underscores the need for reliable tree risk assessment methods that can overcome the limitations of current practice, which often tend to be technically complex and costly, or have proved to be too simple to allow for reliable assessments of the actual safety factors involved.

1.1. Pulling Tests for Tree Safety Assessment

The pulling test is an experiment that involves applying a static load to the tree while measuring stem strain and stem base rotation. It has been widely used to evaluate the strength of trees in scientific studies for many years [8–11]. The Static Load Test Method or Pulling Test Method sets out to non-destructively estimate the strength of a tree's stem and anchorage and correlate those with wind actions to be expected in a storm in order to establish safety factors against stem or root failure [12–15]. It remains the only available method of advanced inspection to assess ad hoc tree stability in strong winds [16].

1.2. Stem Bending and Strain

Stem bending refers to the deflection of the tree stem under lateral loads, influenced by stem flexibility and structural properties [17–19]. Strain gauges are the most precise and widely used tools for measuring tree bending, providing direct quantification of strain [20–25]. These methods are robust in field conditions and suitable for both static and dynamic measurements. Complementary tools, such as accelerometers, inclinometers, and optical systems, offer valuable data for dynamic sway and frequency analysis [25–30].

During a pulling test, strain gauges measure small changes in fiber length (often at an accuracy of 1 μm) at the stem periphery. These measurements, taken on both the tension and compression sides of the trunk, mirror the tree's response to simulated wind loads and may be correlated to the elastic limit of the fiber to derive critical bending moments that may induce primary failure of the wood fibers. Because the outermost fibers experience the greatest stress during bending, measuring their strain helps estimate failure loads for the tree stem. These measurements allow safety calculations to assess the breaking safety of the stem if combined with wind-load data and material properties of green wood.

1.3. Stem Base Inclination

Stem base inclination, or tilt, describes the rotation of the root–soil plate at the tree base and is a critical indicator of anchorage strength and uprooting risk [3,31,32]. High-precision inclinometers or triaxial accelerometers, attached at the stem base, record basal stem inclination. These devices capture dynamic tilt responses at high sampling rates (e.g., 10–20 Hz) during wind events, static pulling, or quick-release tests [1,28,32–37].

The bending moment required to reach a specific inclination in a pulling test (e.g., 0.25°) serves as a proxy for anchorage strength [14,15,31]. Alternatively, tree anchorage is assessed based on basal inclination in high winds [32,36,37].

1.4. Torsion

Trees experience both bending and torsional vibrations in the wind. Torsional vibrations are most pronounced in the crown and upper branches, particularly under low to moderate wind loads. As wind intensity increases, bending dominates, though torsion remains relevant for localized stress and potential failure points in branches or in the stem at the base of the crown [38]. Common methods for measuring torsion or torque in tree

stems include strain gauge arrays [22,39], gyroscopes and accelerometers [38,40] and digital image correlation [28]. Due to their complexity, these techniques are currently not applied in standard pulling tests for tree assessment.

1.5. Measurement Challenges and Research Needs

The quantitative assessment of tree stability often relies on static pulling tests, which measure strain and basal inclination as indicators of the mechanical response of the stem–root system. However, there are situations in which pulling tests reach their limits. One example is large trees with large-diameter stems and strong anchorage. Their size and rigidity necessitate high applied forces to produce strain and tilt signals of sufficient magnitude to allow for reliable extrapolations. Especially for low signals, the noise of standard sensors overlays the small signal to a degree that may compromise the confidence level of gathered data. Furthermore, the application of such high loads poses safety risks to field teams and surrounding infrastructure, accelerates equipment wear and tear, and restricts testing locations and conditions.

A second example is the assessment of standing dead trees (snags or "ecotorsi") in urban and peri-urban settings. While snags are increasingly retained for their ecological value, their reduced structural integrity results in dead wood fibers at the periphery of the stem and entirely degraded structural roots, making them unsuitable for conventional pulling protocols, which, in order to safeguard non-destructive measurements and to allow extrapolating strength, rely on living marginal fibers [41] and at least some mechanically functional roots [42]. Identifying weak spots where monitoring strains would be essential proves to be difficult for dead trees. Furthermore, at low forces that seem safer for testing these vulnerable stems, many inclinometers and strain gauges exhibit high uncertainty and drift, resulting in poor signal-to-noise ratios. Noisy low-load measurements lead to unstable model fits and inflated error propagation, increasing uncertainty in extrapolated quantities such as critical bending moment or safety factors.

These challenges highlight a methodological gap: field techniques are needed to resolve very small basal inclinations with high precision and little noise in the signal. A higher-resolution approach would enable reliable characterization of the initial portion of the load–response curve and is a prerequisite for robust extrapolations from low responses. It could thus expand the applicability of static tests to both very large trees and structurally compromised snags, given that the robustness of extrapolations from minimal responses on dead and living trees is confirmed by future studies. Early studies gave first hints at the potential of using lasers to track the movement of trees [43].

In addition to pulling tests, the motion of the stem base has been monitored in natural winds to assess tree safety. However, motion-induced accelerations and structure-borne vibration signals can interfere with accelerometer-based angle measurements, often leading to inaccurate tilt readings. This applies to an even greater degree if tilt is measured at higher positions along the stem to derive changes in stem curvature or the bending line of a stem in natural winds. Previously, these interference effects obscured the dynamic response of trees under wind loads. Data evaluation was limited to frequency analysis, because overshooting, signal noise and mathematical integration made displacement calculations highly prone to errors. We addressed these gaps by developing and evaluating a high-resolution, low-noise pulling test method to monitor tree bending, torsion, and inclination under mechanical stress.

We collected data from traditional pulling tests in combination with the new method in two distinct experiments. In the first experiment, we used young, nearly round, and likely homogeneous plantation trees to test the accuracy of the new method, particularly the inclination data collected at the stem base, compared to the traditional method. Since

the curvature of the trunk in this case is directly related to Young's modulus (E), we also compared E estimated from both sets of equipment. A second experiment, which used fragile, dead standing trees, evaluated the usefulness of using multiple lasers along the stem to identify problematic parts of the trunk based on deviations from the theoretical bending line. It also served to collect stem base inclination data with both methods.

As a pilot study, we measured the movement of individual trees in low-strength gusts of wind using the laser method.

2. Materials and Methods

2.1. Trees and Sites

For the first subset, 11 *Pinus taeda* L. (mean height: 19.1 m, mean diameter at breast height (dbh): 0.36 m) and 10 *Platanus* × *hispanica* Mill. ex Münchh. (mean height: 20.6 m, mean dbh: 0.43 m) were pulled to failure at a forest plantation in northern Uruguay in August 2025.

In Göttingen, Germany, 19 standing dead urban trees (11 *Fagus sylvatica* L., 4 *Acer pseudoplatanus* L., 1 *Acer platanoides* L., 1 *Quercus alba* L.) with dbh between 0.36 m and 1.1 m were non-destructively measured in autumn 2025. They had been dead for at least 5 years.

To evaluate the feasibility of measurements under natural wind excitation, a red oak (*Quercus rubra*) in Rostock, Germany, with a dbh of 120 cm and an approximate height of 18 m, was tested under wind gusts of approximately 35 to 40 km h^{-1}. Wind speed was derived from regional meteorological data, as on-site measurements were not available. The tree is located in a cemetery with park-like vegetation: large bushes and mature trees of similar height in its surroundings. In addition, an *Acer spec.* with an open cavity in the trunk was monitored. The tree was part of a north–south avenue, with an unobstructed windward side facing west.

2.2. Pulling Tests

All trees were pulled non-destructively to an inclination of 0.25° at the stem base. The forest trees in Uruguay were pulled to failure in a second pull. During the winching tests, the applied force was measured continuously with a forcemeter (load cell) in the pulling line, while the resulting rotation of the root plate was measured with a bi-axial inclinometer at the side of the stem base. Strain of the outermost fibers was measured using four strain gauges installed at equidistant points between 1 m and 4 m on the side of the stem under compressive stress. Further inclinometers were installed at heights of 2 m and 5 m.

The instruments used are part of the TreeQinetic system (IML Electronic GmbH, Rostock, Germany). The inclinometers had a resolution of 0.01° (quasi-static motion, with an accuracy of 0.02°), the strain gauges had a resolution of 1/10,000 mm (with an accuracy of 1/1000 mm), and the forcemeter had a resolution of 0.1 kN (with an accuracy of 0.3 kN). The rope angle from the horizontal was measured by an on-board inclinometer in the forcemeter. The test was configured according to the Static Load Test Method or Pulling Test Method [44]. The applied force was converted into its lateral component using the cosine of the rope angle. The bending moment was determined by multiplying the lateral force component (in kN) by the lever arm length, which was measured as the vertical distance from the respective sensor's position to the anchor point of the rope (in meters).

Prior to testing, tree crowns were removed from forest trees to eliminate the influence of the unknown weight of the crown and to prevent errors caused by wind impact or branches getting caught in adjacent trees.

2.3. High-Resolution Pulling Test Method with Laser Deflectometer

2.3.1. Material

For optical measurements of tree responses to applied loads, the LOFOR® Laser Deflectometer (Engineering Firm for Tree Inspection Technologies, Rostock, Germany) was used. The system consists of multiple long-range laser units mounted on the tree using precision mechanical alignment mounts, as well as a camera support system—typically holding a smartphone—and a semi-transparent projection screen. These components are arranged on purpose-built stands to ensure stable positioning and optical alignment.

2.3.2. Experimental Set-Up

For measurements using the laser deflectometer introduced here, laser emitters were mounted at multiple heights along the stem. Unless noted otherwise, the bottom laser was mounted at the stem base, while four other lasers were installed at 0.5, 1.0, 1.5 and 2 m height, respectively. The laser beams were precisely aligned to strike a semi-transparent projection screen positioned between 5 and 12.5 m from the tree, which was recorded from the rear by a camera (Figure 1). This distance was exactly 5 m for the ecotorsi, but, due to the difficult terrain, it was variable in Uruguay. The distance was measured with a laser distance meter (LD080P, Makita, Ratingen, Germany). Thus, any movement of the stem was transmitted instantaneously by the laser beams onto the projection screen and recorded, allowing contact-free and delay-free detection of stem displacement.

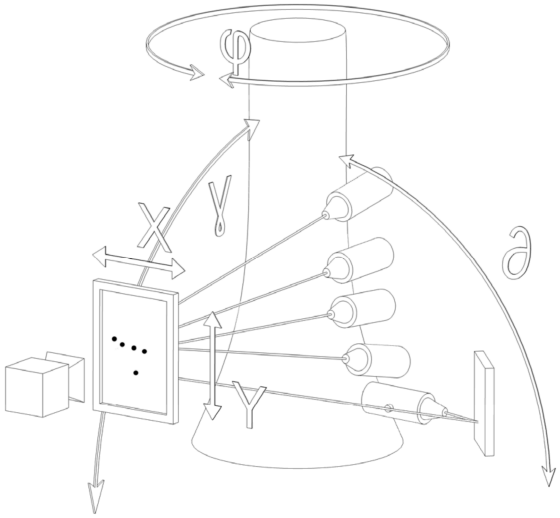

Figure 1. Camera, projection screen, laser emitters. X and Y: Coordinates of laser dot movement on the screen. γ denotes the inclination in the direction to or away from the screen, φ is an angle related to either a rotation around the stem axis or to a stem tilting sideways. ∂ denotes the angle perpendicular to γ. This angle is detected by the lowest laser, whose beam is directed onto the screen by a mirror.

The video was analyzed with custom software to determine the vertical and horizontal displacement of the laser beams during the experiment in X and Y directions and to calculate the respective changes in angle of the laser beams from the distance between lasers and screen. The temporal resolution of this method therefore depends on the frame rate, which is set to between 24 and 60 Hz depending on the camera model and experimental setting, while the spatial resolution is affected by the distance between the laser and the screen as well as the resolution of the video.

2.4. Theory of Stem Response Measurements with Laser Deflectometer

The method exploits a fundamental geometric principle: the intercept theorem (principle of similar triangles). By increasing the distance between the tree and the projection screen, the resolution of the measurement results can be adjusted almost arbitrarily—at least to the extent permitted by the topographical and structural surroundings of the tree. The nature of a laser beam ensures a delay-free and distortion-free amplification of the tree's movements. The actual rotation of the laser beams, and thus the deflection of the section the lasers are attached to, can be derived by applying the intercept theorem to the displacements of the laser points recorded on the screen. The method can only be used to measure rotational movements in which the laser beams are directed perpendicular to the axis of rotation.

In a load test, for example, this corresponds to the pulling direction, as the tree rotates around an imaginary axis in the root zone that is perpendicular to the applied tensile force. In Figure 1, this is shown by angle γ.

Torsional rotation of the stem about its longitudinal axis under natural wind excitation (Figure 1, angle φ) also fulfils the geometric conditions of the intercept theorem. Consequently, torsional angular displacements are geometrically amplified in the projected laser-point movement. With the current setup, it is impossible to unequivocally partition the displacement along the x-axis into torsion and oblique bending.

2.4.1. Laser-Point Movement in One-Axis Pull Tests

Stem bending in the direction of the laser beam results in a vertical displacement of the laser points on the projection screen. According to the intercept theorem, this displacement corresponds directly to the stem inclination angle at the point of laser attachment. In analogy to the conventional pixel coordinate system used in digital image analysis, these angles measured along the y-axis of the screen are denoted as γ in this study.

2.4.2. Laser-Point Movement in Natural Sway Motion

If the tree additionally deflects in a direction not parallel to the direction of the laser beam, i.e., sideways or in torsion, this motion is represented as a horizontal displacement of the laser points on the projection screen. These horizontal displacements are referred to as "x" in this work. For bending movements perpendicular to the laser beam direction, the intercept theorem is not applicable. The measured x-displacements therefore do not represent geometrically amplified angles; rather, depending on the direction of motion, they might correspond approximately one-to-one to the actual tree displacement.

In contrast, if the stem undergoes torsion around its longitudinal axis, the intercept theorem applies. Therefore, the measured x-displacements presumably mainly represent torsional displacement with some involvement of bending perpendicular to the load direction (oblique bending). To distinguish between torsional motion and oblique bending in the x-displacement of the laser beam, a second laser directed orthogonally to the first must be introduced (Figure 1, lowest laser).

Any inclination of the bottom laser, caused by the load, directly represents the rotation movement of the stem base. This inclination should be equivalent to that measured by the inclinometer installed at the same height.

2.4.3. Estimates of the Modulus of Elasticity

Flexural stiffness, the product of Young's modulus and the cross-section's moment of inertia, can be derived directly from the bending line of a cantilever beam by relating the beam's curvature to the applied bending moment from fundamental beam theory. As in previous studies, the bending angle of a respective section of the stem is determined

by subtracting the inclination below the section from the inclination measured above [41]. This also applies to the root system as its rotational movement is captured by the bottom laser. The fundamental relationship is expressed by Euler's Elastica theorem, which states that the curvature κ at a point in the beam is proportional to the bending moment M at that point:

$$\kappa = \frac{M}{EI} \tag{1}$$

E is the modulus of elasticity, and I is the moment of inertia of the beam cross-section. This applies under the basic assumption that $\kappa d \ll 1$, where d is the beam diameter. For a cantilever beam, a beam that has only one support in the form of a fixed bearing, the angle α of maximum deflection can be calculated as a function of the beam length l as follows:

$$\alpha = \frac{Ml}{EI} \tag{2}$$

This approach is considered a sufficient model and state of the art in beam theory [45]. Figure 2 shows the measured variables during the experiment.

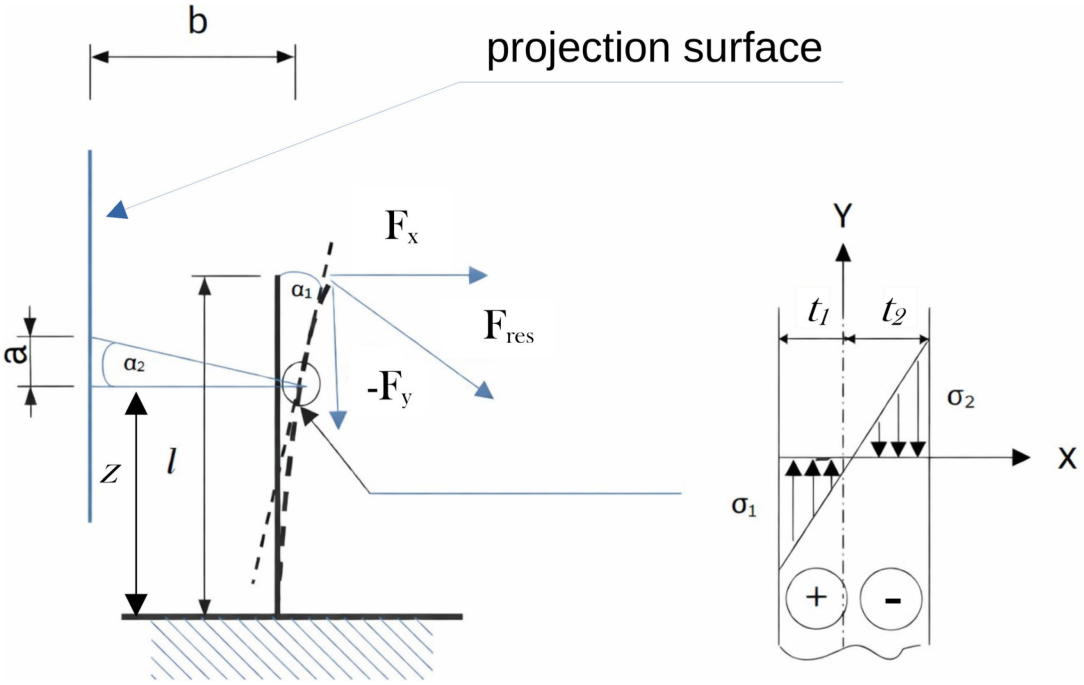

Figure 2. Illustration of the measured and derived physical quantities in the experiments. Cantilever beam of length l, F_{res} applied force at the free end, F_x axial component (small influence on bending), F_y transverse component (causes bending), support at $y = 0$, a and b are the displacement of the laser dot on the screen and distance between laser and screen, respectively, used to calculate angle α_2, corresponding to the slope produced by F_y. The dashed line is the bending line. The angle is the tangent slope. σ_1 and σ_2 are the bending stresses that reach their maximum at t_1 = max and at t_2 = max. Further explanation in text.

For classic cantilever beams with end force, we can estimate the modulus of elasticity E from their curvature in bending [46–57]:

1. Bending moment distribution of a cantilever beam

For a cantilever beam with an end force component F_x acting perpendicular to the beam axis, the bending moment is given by:

$$M(z) = F_x(l - z) \tag{3}$$

where

- F_x = force component perpendicular to the beam axis
- l = total beam length
- z = distance from the fixed support (ground level)

2. Beam differential equation

Using the Euler–Bernoulli beam equation:

$$EI\frac{d^2\omega}{dz^2} = M(z) \tag{4}$$

where $\omega(z)$ denotes the lateral deflection of the beam in the x-direction.

Substitute the bending moment:

$$EI\frac{d^2\omega}{dz^2} = F_x(l - z) \tag{5}$$

3. First integration (beam slope):

Integrating once yields the slope of the beam, defined as $\frac{d\omega}{dz}$:

$$EI\frac{d\omega}{dz} = F_x\left(lz - \frac{z^2}{2}\right) + c_1 \tag{6}$$

Boundary condition at the fixed support:

$$\frac{d\omega}{dz}(z = 0) = 0$$

Therefore

$$c_1 = 0$$

and

$$\alpha_1(z) = \frac{F_x}{EI}\left(lz - \frac{z^2}{2}\right) \tag{7}$$

This is the rotation angle of the beam at position z. This solution is valid under the assumption of a constant bending stiffness EI along the beam. For trees, where neither E nor I can be considered constant, this implies that the result of the application of this solution renders estimates of an apparent E if the cross-sections are of regular shape. In cases where the shape of the cross-sections is inhomogeneous in the tested part of the tree stem, the laser deflectometer allows an estimate of an effective EI that illustrates the bending behavior of the stem.

4. Relation to the optical measurement:

In this method, the angle is determined using a projection method.

From the geometry:

$$\tan(\alpha_2) = \frac{a}{b} \tag{8}$$

where

- a = displacement on the projection surface
- b = distance to the projection surface

Since the rotation angles occurring in the bending experiment are very small, the small-angle approximation can be applied:

$$\tan(\alpha_2) \approx \alpha_2$$

Hence, the rotation angle of the beam can be obtained from the measured displacement on the projection surface:

$$\alpha_2 \approx \frac{a}{b}$$

For discrete measurement points along the stem, the angle at position y_i is given by

$$\alpha_{2,i} \approx \frac{\alpha_i}{b}$$

where a_i is the measured displacement on the projection surface and b is the distance to the projection plane. Since the rotations are small, the optically measured angle corresponds to the mechanical slope of the beam:

$$a_{1,i} \approx a_{2,i}$$

For small rotations, the optically measured angle α_2 can be assumed to be equal to the mechanical slope α_1 of the beam at the same position. This allows the measured angles to be directly related to the beam mechanics.

The mechanical behavior of the beam is described by the Euler–Bernoulli equation:

$$\frac{d\alpha_i}{dy} = \frac{M(y)}{EI(y)} \tag{9}$$

If the bending stiffness varies along the stem, analytical integration is no longer valid. Therefore, the equation is evaluated incrementally between two neighboring measurement points:

$$\alpha_{1,i+1} - \alpha_{1,i} = \frac{M(y_i)}{EI(y_i)}(y_{i+1} - y_i)$$

Substituting the measured angles yields:

$$\alpha_{2,i+1} - \alpha_{2,i} = \frac{M(y_i)}{EI(y_i)}(y_{i+1} - y_i)$$

The bending moment at position y_i is given by the horizontal force component:

$$M(y_i) = F_x(l - y_i)$$

Solving for Young's modulus results in:

$$E(y_i) = \frac{F_x(l - y_i)}{I(y_i)} \frac{y_{i+1} - y_i}{\alpha_{2,i+1} - \alpha_{2,i}} \tag{10}$$

Finally, inserting the optical relation leads to an expression based purely on measured quantities:

$$E(y_i) = \frac{F_x(l - y_i)}{I(y_i)} \frac{(y_{i+1} - y_i)}{\alpha_{i+1} - \alpha_i} b \tag{11}$$

In tree stems, E cannot be considered constant between two laser positions. Likewise, I may significantly vary in irregularly shaped stems as the diameter and form of the cross-section change. Therefore, for stems with a regular shape, the result of Equation (11) is an apparent E. If the stem section between two laser points has an irregular shape, an effective stiffness EI may be calculated based on Equation (11) instead.

E from elastometer data was calculated from the slope of the regression of stress on strain, assuming an elliptical cross-section of the trees, calculated from two diameters measured parallel and perpendicular to the load direction at the height of each sensor. Bark thickness was estimated after the trees were sectioned for further analysis.

The same assumption of an elliptical cross-section and the bark thickness measurements in the field were used to estimate the second moment of inertia I for the E estimate from laser data. E at the midpoints between adjacent lasers was then estimated from Equation (11) using the vertical displacement a with respect to the section below at peak force F.

2.5. Bending vs. Tilting

The ratio of stem strength to root system anchorage should be reflected in the different rates at which angles change at various heights along the stem during the experiment. We tested the hypothesis on 19 ecotorsi: a tree with a strong stem and weak roots should tilt without bending much, while a well-anchored tree with a stem defect should bend without tilting much.

2.6. Torsion and Oblique Bending

Torsion and oblique bending are recorded as horizontal displacement of adjacent laser beams. However, since the Intercept Theorem applies only to torsional displacement and not to oblique bending, the greater magnitude of the measured horizontal displacement (x) is most likely caused by torsion. At the stem base, the displacement of the laser beam could also result from a sideways component of tilt, which is often observed in pulling tests due to the inhomogeneous structure of the root–soil matrix. With the setup used for the experiments reported here, however, these two types of displacement cannot be separated.

2.7. Data Analysis

Data were analyzed using R 4.5.2 [58].

3. Results

3.1. Validation: Correlation of Traditional and New Inclination Measurements

Basal inclination measured with both methods generally agreed well, with coefficients of correlation exceeding 0.98 (mean 0.90, s.e. 0.05) in most cases, although some trees showed systematic deviations (Figure 3). The slope of the regression of laser inclination against inclinometer inclination was 1.0 ± 0.001 (s.e.) for all 41 measurements pooled together.

3.2. Correlation of Traditional and New MOE Measurements

Apparent E from strain gauges and curvature was in the same range of 1 to 5 GPa but did not correlate (Figure 4).

3.3. Bending vs. Tilting

Multiple lasers along the stem allow analysis of the bending behavior under load at a level of detail that was not possible so far in the usual type of pulling tests. The data of the ecotorsi demonstrate three different types of reaction from these trees during loading (Figure 5). The values displayed here indicate the difference in inclination between two adjacent lasers along the stem, while the bottom laser indicates the rotation of the stem base. The trees in panel A just tilted at their base, adding only small amounts of inclination due to bending in the stem. Trees in panel B tilted and bent at their base, while trees in panel C bent most in the lower section and turned out to be stiffer at the top of the monitored section.

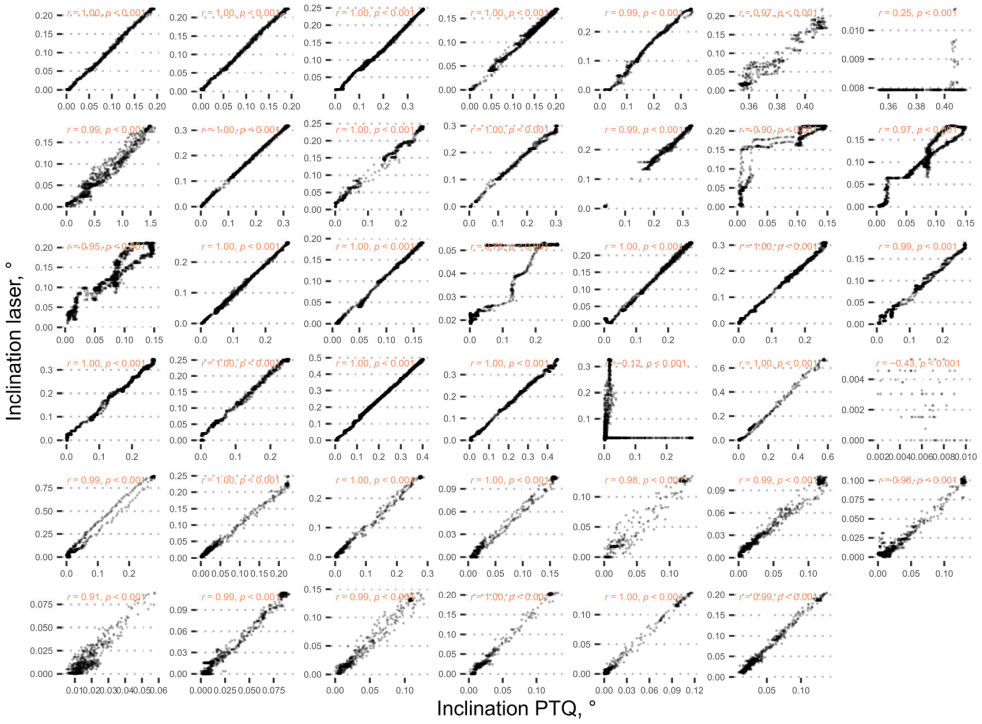

Figure 3. Correlation of stem base inclination measured with an inclinometer (PTQ) and the new laser system. Data from plantation trees in Uruguay (first 21 panels) and ecotorsi in Germany.

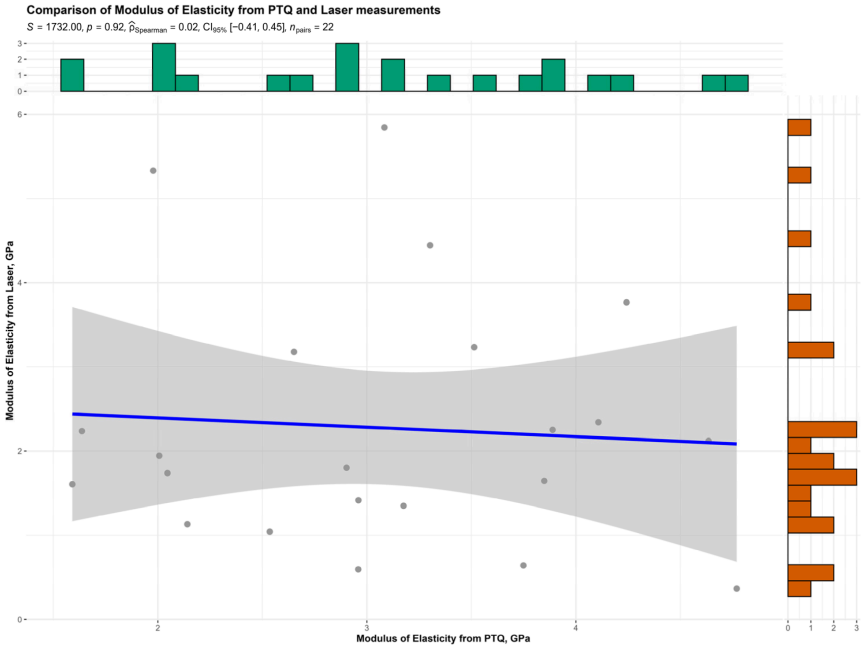

Figure 4. Correlation (blue line) between apparent MOE derived from traditional strain gauges (PTQ) and new laser measurements. Marginal bar charts: frequency distributions of laser (red) and PTQ (green) data.

3.4. Torsion and Oblique Bending

The ecotorsi showed a distinct pattern of lateral movement. While most stems did move strictly towards the screen, some trees did move noticeably left or right. Without a second, perpendicular set of lasers, the final interpretation must remain open. However, we would assume that a tree with torsion or oblique bending would have a constant rate of moving sideways across all heights. The unequal spacing of the left tree in Figure 6

indicates that we may interpret the data as indicating torsion or oblique bending. While the top laser of one tree made no lateral movement (Figure 7, green), the direction of the top laser of the other tree changed by more than 0.3° (Figure 7, red). This is, however, only correct in the case that it was pure torsion.

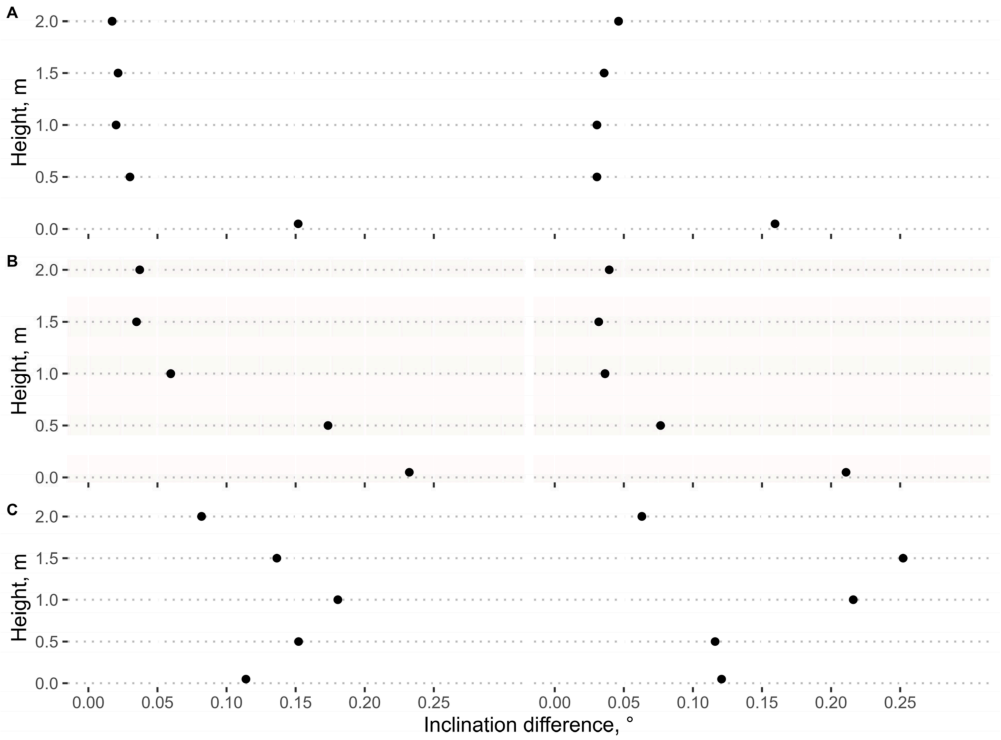

Figure 5. Results of six trees that we interpret as three types of bending and titling in ecotorsi. (**A**) Stem is only tilting at the stem base; (**B**) Lower 0.5 m are tilting and bending; (**C**) Significant stem bending. Data points show differences in angles between adjacent lasers at maximum basal inclination. Height is installation height of lasers above ground level.

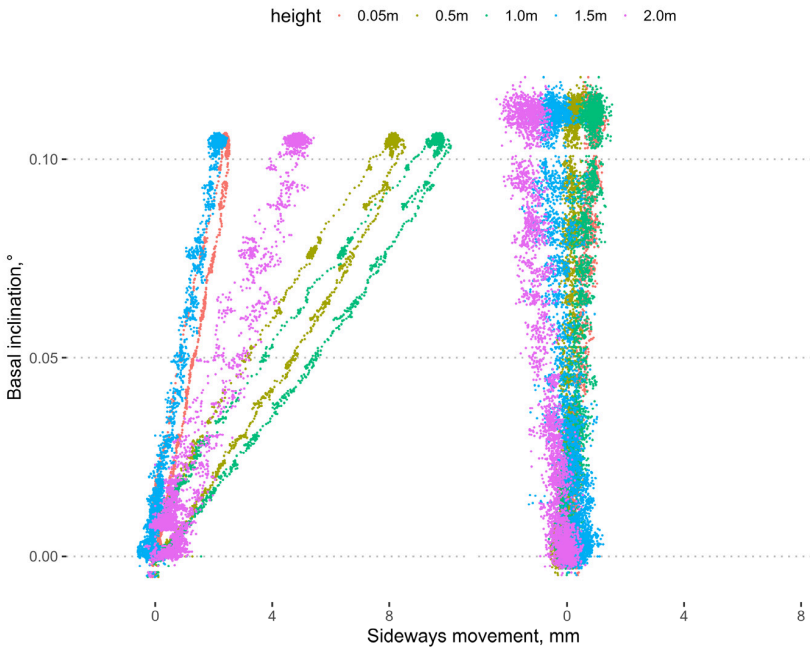

Figure 6. Two ecotorsi with a distinctively different pattern of lateral movement. Data of the same trees as in Figure 7 below, but interpreting the observed changes as sideways movement (difference between adjacent lasers) instead of torsion.

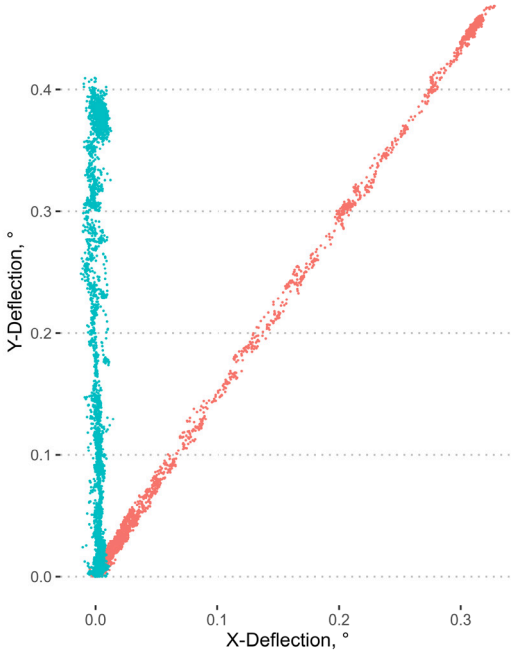

Figure 7. Twisting or oblique bending at 2 m height above ground level in two ecotorsi. Both trees were pulled in the y-direction. x-deflection is only valid if it was caused by torsion only.

3.5. Variance

The RMSE of a standard model that describes the relationship of force and inclination [59], fitting the laser data to the basal bending moment was less than a third of a similar model for the inclinometer measurements, indicating significantly lower variation (Figure 8).

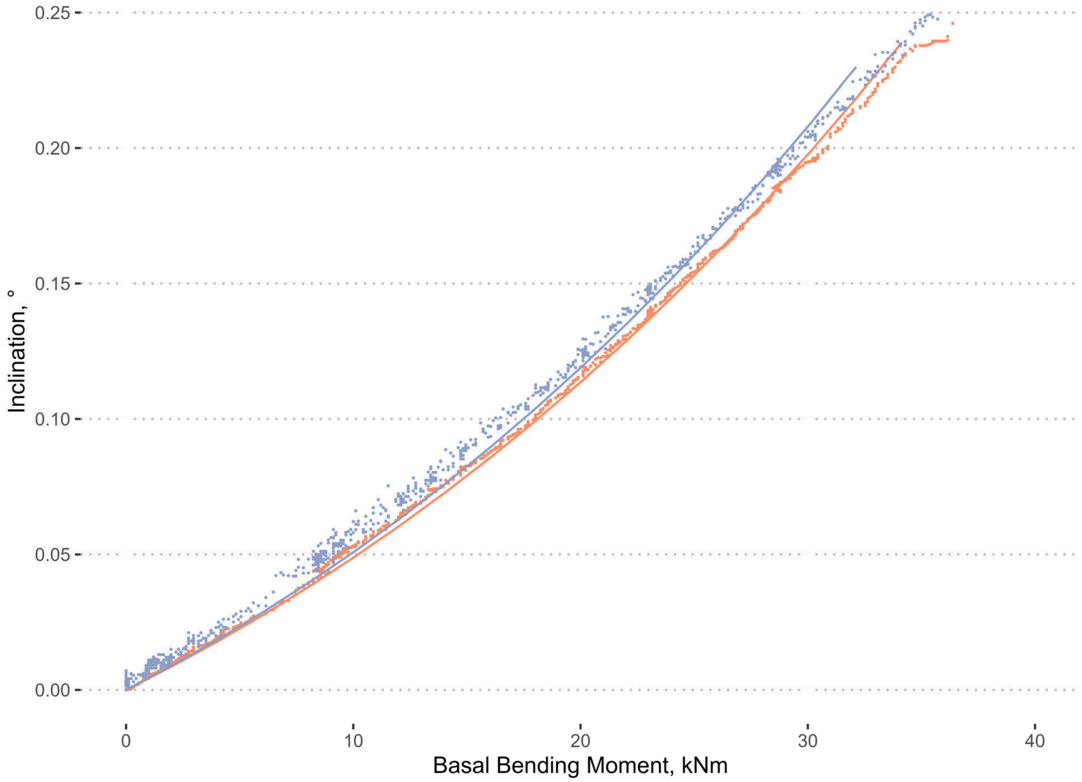

Figure 8. Comparison of the inclinations measured with inclinometers (blue) and lasers (red) for a pine tree. Lines are fitted as described in [59].

The angle estimation algorithm proved to be quite resistant to errors in the input data. Deviations from the true distance between lasers and the screen change the estimated y-angle by an equivalent proportion, i.e., a 10% error in distance translates to an approximate error in angle of 10% (Figure 9).

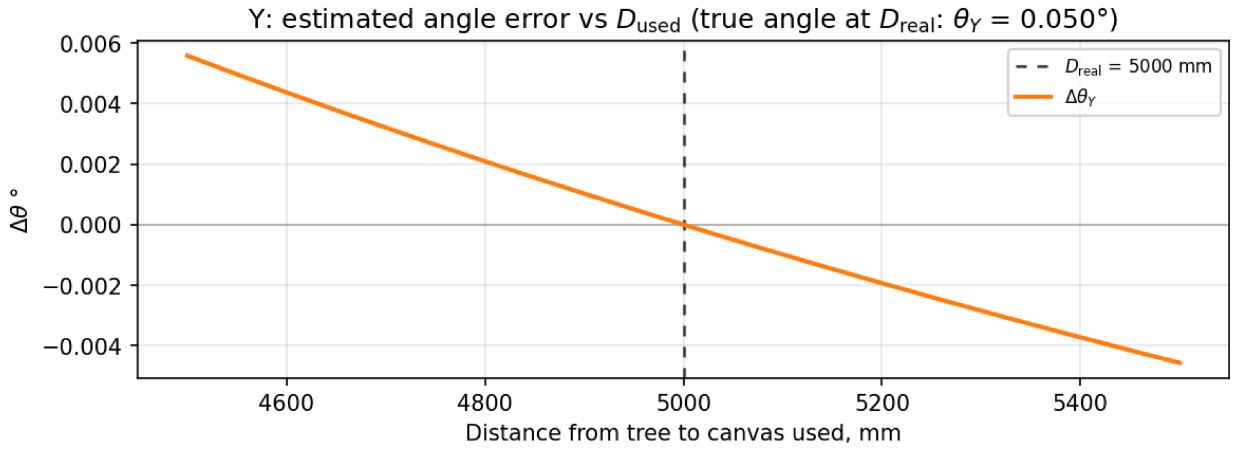

Figure 9. Effect of deviations between the true distance to the screen (here: 5 m) and the measured distance used for angle calculations on the estimated stem base inclination, shown as deviation from the true angle.

3.6. Sway Motion of Trees in Wind

For the measurement of the *Q. rubra* in natural wind, the lasers were aligned with the prevailing wind direction to capture the dominant inclination component (*y*-axis) corresponding to wind-induced loading. Stable inclination measurements with a resolution better than 1×10^{-3} degrees were achieved (Figure 10). Higher-frequency components observed in the signal do not represent structural vibration modes of the tree but arise from limitations of the video-based tracking procedure.

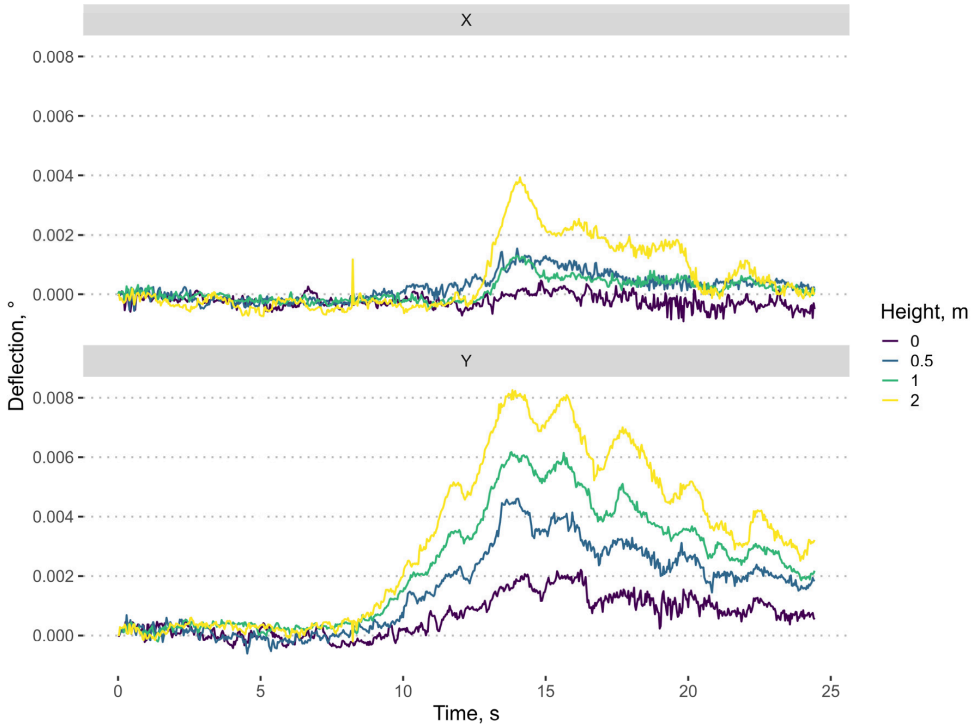

Figure 10. Deflection of a large *Quercus rubra* (dbh 1.2 m) in a gust of ~40 km/h. Top: x-direction (left/right), bottom: y-direction (towards/away from screen).

Figure 11 shows the movement of a tree with a substantial open stem cavity above the second laser. Deflections in x (left–right) and y (towards and away from the camera) are highly correlated (R^2 = 0.89), but slopes differ significantly ($p < 0.001$) between the two lasers below the cavity and the two upper lasers. While the available data do not allow us to determine to what degree one or the other representation, or a mixture of both, was true, they qualitatively help to locate the damaged part of the stem.

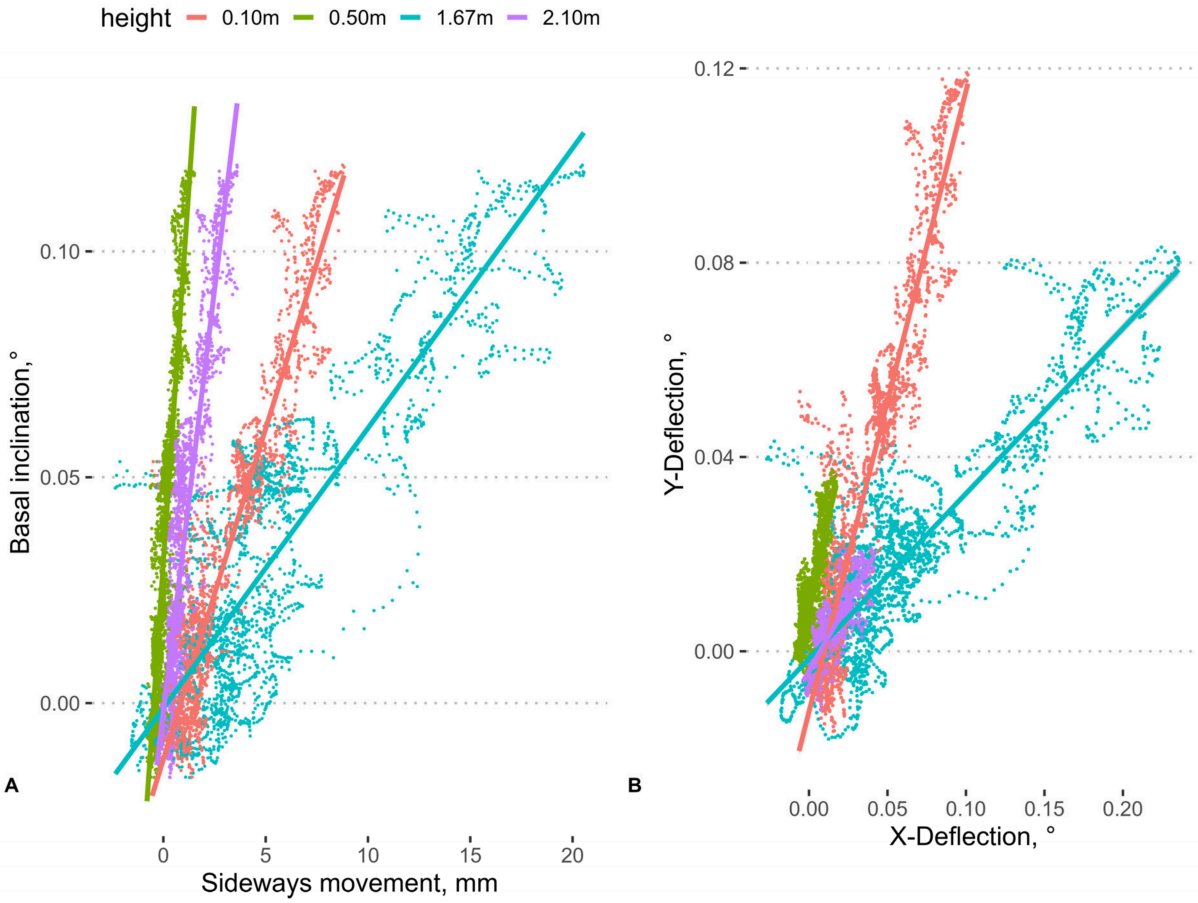

Figure 11. Two representations of the same data of an *Acer spec.* tree in natural wind. There was an open cavity between the two lower and two upper lasers. (**A**) Horizontal movement (difference between adjacent lasers) of lasers as sideways motion. (**B**) Deflection. Data points show differences between adjacent lasers. Lines: linear regression.

4. Discussion

The evaluation of pulling tests is based on extrapolating the relationships between inclination, strain, and applied bending moments within the non-destructive range until failure occurs. If the tree is fragile, the forces must be limited to prevent overloading its weakest part. Consequently, the resulting strain or stem base rotation may be very small, and the signal-to-noise ratio may be very low. Furthermore, the standard instrumentation used in these tests provides measurements at only a limited number of discrete points along the stem; in the worst case, only one point is measured at a time. Consequently, assessors face two major challenges. First, trees may be too fragile to withstand the forces required to produce meaningful inclination data at the stem base. Second, it becomes increasingly difficult to identify the structurally weakest location in large, old, compromised trees using point-based measurements. Therefore, there is a need for a method that allows such trees to be monitored using lower forces with more sensitive instruments that record the inclination response at the stem base more precisely. At the same time, higher spatial coverage is

required to fully monitor the tree's response to applied loads and avoid overloading its load-bearing structure, in case the weakest spot was not equipped with a sensor.

In contrast to the established methods, the laser deflectometer measures the deflection of an entire stem section rather than isolated points on the trunk. Stem deflection reflects the combined effects of trunk geometry, spatially variable wood properties, and—where present—internal damage. In this sense, stem bending represents the integrated mechanical response of all structural features of the trunk. At the same time, a laser at the stem base can provide data to assess the anchorage strength of the tree at a high resolution.

We hypothesized that laser-based monitoring of tree movement would yield high-resolution data on:

- Deflection across a continuous portion of the stem;
- Stem base inclination.

Using lasers as proposed in this study addresses the shortcomings of previous approaches in several ways:

- In contrast to inclinometers, lasers do not confound the effects of motion-borne acceleration and inclination.
- The measurement principle we propose allows the resolution to be increased almost infinitely.
- The data from all lasers are synchronized precisely in terms of time. This allows for the accurate examination of dynamic processes of the tree's stem motion.
- Sampling rate depends on the frame rate of the camera and typically ranges between 30 and 60 Hz. That data rate is well suited for monitoring tree sway motion in wind as well as short pull-force impulses generated by hand, which is sufficient for smaller trees.
- There is no instrument drift caused by temperature changes.
- The proposed set-up can monitor bending at several points along the basal 2 m of the stem.
- The application of the laser deflectometer may be constrained by site conditions, as the method requires an optically unobstructed distance of approximately 3–10 m between the tree and the projection screen.

We used a series of experiments to validate the data of the new method with concurrent measurements using standard legacy instrumentation.

4.1. Inclination and Bending Line

Inclination data of the new method correlated very well with inclinometer measurements but with significantly reduced scatter (Figure 3). The range of angles and the shape of the relationship between bending moment and basal angle agreed well with data in the published literature [31].

Triaxial accelerometer-based inclinometers are susceptible to temperature drift, which can distort the inclination signal and potentially undermine stability assessments if undetected. Therefore, sensor zeroing is essential for accurate data post-processing in the inclinometer method. In contrast, the laser deflectometer method tracks beam positions relative to their initial location during analysis, eliminating the need for a separate zeroing process. Additionally, laser-based signals are insensitive to temperature variation and exhibit significantly reduced susceptibility to vibration and electronic noise.

Thus, temperature drift is a potential explanation for the deviations between laser measurements and inclinometer data. Additionally, inhomogeneous root systems might have affected measurements at specific positions because devices could not be installed at the same spot of the tree. This is why multiple measurements are always required in practice.

The analysis of the bending line of the dead tree stems under load resulted in a set of possible indicators, which might allow for a more detailed assessment of trees in the future (Figure 5). An ecotorso that does not bend but only tilts at the base might be more likely to fail in the root system, while an ecotorso with a distinct kink in the stem bending line might break there. Indeed, during our experiments, one of the trees we tested broke at this kink unintentionally. Tilting at the base, combined with bending in the lower 50 cm, might indicate the typical failure of dead trees that often occurs at their stem base as a combination of uprooting and fracture, sometimes involving along- and across-grain crack propagation in dry or decayed wood.

4.2. Twist and Turn

The model used to evaluate stem strength in pulling tests [13,14] presumes the pull to be strictly unidirectional. Therefore, the tree should bend without any torsion. However, whether these requirements are met could not be measured in standard pulling tests until now.

Some of the trees we pulled did indeed show signs of oblique bending or torsion. Currently, these two effects cannot easily be distinguished. To address this better, we added another set of lasers at right angles to the original set (Figure 12). This will allow us to monitor the movement of trees comprehensively, so that torsion and oblique bending can be distinguished. It should be noted, however, that torsion is unlikely to have a significant impact on tree stem failure [38].

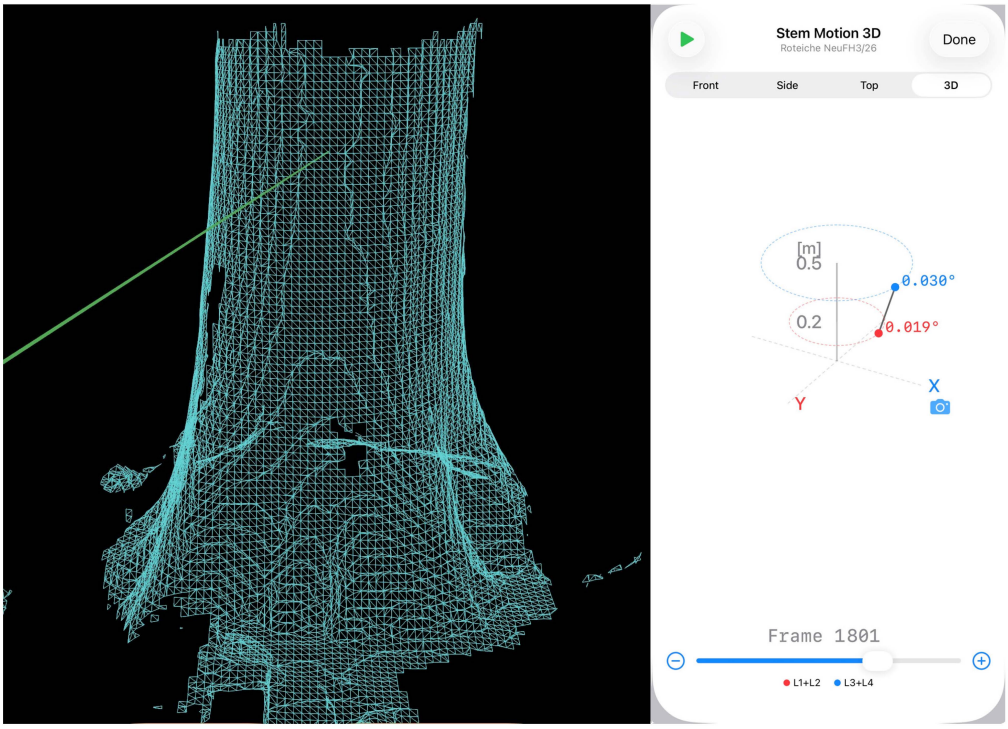

Figure 12. Two screenshots of the current app. The green line represents the camera position. (**Left**) 3D model of the trunk based on a LiDAR laser scan. (**Right**) Angle of inclination and direction of inclination of the two lowest laser positions, each of which was equipped with two lasers. The camera icon on the *x*-axis represents the position of the screen; the *y*-axis shows the direction in which the secondary lasers are pointing.

Besides helping to preserve valuable old trees, this new method could also advance our knowledge about these trees, because it allows us to measure torsion and oblique bending with simple low-cost instruments.

4.3. Deviation of Modulus of Elasticity from Both Methods

The apparent modulus of elasticity (E) measured in bending a living tree assumes that the stem behaves as a linearly elastic, homogeneous, orthotropic beam with small deflections, negligible shear (for large L/h), ideal supports and loading, fixed bearing, and minimal time-dependent effects. However, several factors can cause deviations from these assumptions and thus bias E estimates. The main sources of deviation reported across studies of wood and trees include unmodelled shear deformation, spatial heterogeneity (e.g., knots, fiber angle, and ring structure), strong anisotropy, and non-ideal boundary conditions [60,61]. These deviations can cause the measured E to differ systematically from ideal theoretical predictions and may have affected the two methods used in this study differently, potentially explaining some of the observed differences in results.

Notably, the assumed constant diameters for a specific section, the section's ideal elliptical shape, and the estimated uniform bark thickness all influence the relevant net diameters and shape used to calculate the moments of inertia (I). While these factors can greatly affect E, the same I was used for both methods in this study, so they cannot explain the differences between the two methods (Figure 4).

4.4. Sway Motion of Trees in the Wind

In previous research [62,63], different sensor technologies were used. The use of accelerometers—often referred to as inclinometers because they derive tilt angles from gravity measurements—to monitor tree root stability under wind loading was investigated in [32,36,37,63]. This method proved effective for identifying trees with weak anchorage, particularly when wind gusts of at least 50 km h^{-1} occurred during the monitoring period. Higher wind speeds generally produced clearer signals; however, they also introduced numerous secondary effects, complicating data interpretation. Furthermore, information on stem structural weaknesses could not be reliably derived from accelerometer data. Another limitation was the limited temporal synchronization accuracy among multiple inclinometers mounted at different heights along the trunk.

In contrast, the high sensitivity of the laser deflectometer method enables detailed monitoring of tree motion during low-wind events. Unlike accelerometer-based approaches, laser deflectometer data allow simultaneous analysis of both root plate tilt and stem structural soundness. Measurement accuracy can be readily enhanced by increasing the distance between the tree and the projection screen, thereby amplifying laser-point displacement without increasing applied loads.

Our controlled pulling tests demonstrated a tight relationship between applied force and laser-measured tilt—even at very low loading (Figure 8)—and preliminary measurements on two trees in natural wind showed promising data at low wind speeds (Figures 10 and 11). Thus, even trees of this size might be reliably assessed under low-wind conditions using this method.

The minor oscillations are attributed to imperfections in the video-based analysis rather than to biomechanical tree responses. These artifacts arise from limitations in frame-to-frame laser-point detection and from minor screen and camera movements caused by wind. As these effects occur at frequencies and amplitudes inconsistent with known tree dynamic behavior, they can be clearly distinguished from mechanically meaningful signals and do not affect the interpretation of stem inclination or structural response.

4.5. Implications of Findings

The new method could significantly improve tree risk assessment in urban environments. By providing higher-resolution data with greater accuracy and the ability to measure torsion and oblique bending, this method offers a more comprehensive understanding of

tree biomechanics. Therefore, it is suitable for improving current methods of assessing tree stability or the likelihood of stem fracture. For example, it may provide users of the Static Load Test Method with additional information to check if the test data are plausible and the results of their evaluations are reliable. This could be particularly useful in urban forestry, where the stability of trees is crucial for public safety.

4.6. Practical Applications

4.6.1. Anchorage

The correlation between the applied load and the resulting tilt at the stem base is nonlinear [31]. Therefore, extrapolations of the anchorage strength required by the Static Load Test Method can suffer from large scatter in the data. This is especially true when only a few data points are evaluated. At very low inclinations, the resolution of current inclinometers is insufficient to derive reliable correlations between the applied load and the resulting inclination. The laser method can significantly improve this issue.

To date, research has only confirmed a strong correlation between rotational stiffness at 0.25° inclination at the stem base and loads at uprooting failure, as proposed by [14]. The greater resolution and higher precision of the data gathered using the laser method presented here may allow us to test whether extrapolations can be reliably based on much lower stem base rotations. This could inform future extrapolation algorithms. In the long term, this would enable testing of trees at lower loads than the current Static Load Test Method allows.

4.6.2. Stem Strength

In the Static Load Test Method, laser measurements can be used to verify elastometer data collected at various points along the stem. This is done by comparing the strain levels recorded at individual points with the strain levels generally required to produce the bending line derived from laser measurements at specific stem diameters. Thus, laser data can validate the findings from elastometer readings and prevent the misinterpretation of stem strength. Adding information on oblique bending or torsion during the pulling test could improve our understanding of the underlying biomechanical processes reflected in the test results.

4.6.3. Dynamic Measurements

Furthermore, this method could be applied to various real-world scenarios. Besides static pulling tests, it could be especially valuable when applied to monitoring the motion of trees in natural winds because it allows meaningful data to be collected at lower wind speeds and on the complex responses of living trees. As a simple, low-cost method, it could further our understanding of how tree stems respond to natural wind, which often involves straight or oblique bending, torsion, and tilt. Accurate signals allow for more reliable calculations of the work involved in stem bending and tilting. This improves descriptions of the complex energy transfers involved in the interaction between trees and wind. This will be a significant step forward in understanding wind loads acting on trees.

4.7. Limitations and Future Directions

Directing the lasers at the screen proved challenging on very bright days because the lasers are low-powered to ensure safe operation in busy urban environments. In such situations, it is recommended that the screen be shaded. Sometimes, buildings or vegetation prevented optimal equipment placement. Simple technical solutions are possible when buttress roots or nearby vegetation block ground-level laser beams. For example, one solution is to use laser mirrors to divert the beam. Because the distance between the trees and the screen was rather low in the experiments presented here (around 5 m in most

cases, rarely reaching 10 m), future experiments might easily increase the resolution even further by increasing this distance.

The optical laser method is sensitive to distortion by rain; if testing during rain is required, dedicated weather protection should be installed.

For the experiments presented here, a forcemeter from the PTQ system was used, which had an irregular sample rate. A significant portion of the scatter in the data was likely caused by synchronizing the force and laser data. Therefore, the logged forcemeter data should be better integrated into the evaluation process.

To achieve full two-dimensional tilt characterization, an additional set of lasers oriented perpendicular to this axis would be necessary. Future research could focus on experiments with lasers perpendicular to those used in the reported study. This would enable differentiation between oblique bending and torsion (Figure 12).

Future analyses should consider the actual shape of tree stems. While the plantation trees in Uruguay were almost perfectly elliptical, most urban trees are not. However, creating 3D models of trees using photogrammetry or LiDAR has become very accessible in recent years. These methods allow us to use the true cross-sectional shape of the stem in the analysis (Figure 12).

5. Conclusions

The new laser-based method of monitoring tree movement addresses several shortcomings of the sensors used in traditional pulling tests. Its higher sensitivity allows the acquisition of high-resolution, low-scatter data and the ability to measure torsion and oblique bending. These improvements could enhance our understanding of tree biomechanics and improve tree risk assessment in urban environments. Continued research in this area is essential to further refine and validate the method.

Author Contributions: Conceptualization, S.R. and A.P.C.-D.; methodology, S.R., A.D., B.S., and L.G.; software, S.R. and L.G.; formal analysis, S.R.; fieldwork, S.R., A.P.C.-D., J.L. and A.S.; resources, S.R. and A.P.C.-D.; data curation, S.R.; writing—original draft preparation, S.R.; writing—review and editing, A.D., J.L., B.S. and S.R. All authors have read and agreed to the published version of the manuscript.

Funding: This research was funded by Comisión Central de Dedicación Total of the Universidad de la República and SAG Baumstatik e.V. The APC was funded by HAWK.

Data Availability Statement: Data are available upon reasonable request.

Acknowledgments: The authors acknowledge the support provided by FYMNSA in conducting the experiment in Uruguay.

Conflicts of Interest: Lothar Göcke is the owner of the engineering firm that develops and markets the laser hardware and software used in this research. The remaining authors declare that the research was conducted in the absence of any commercial or financial relationships that could be construed as potential conflicts of interest.

Abbreviations

The following abbreviations are used in this manuscript:

dbh	Diameter at breast height
E	Modulus of elasticity
F	Force
I	Second moment of inertia

References

1. Yang, Z.; Hui, K.W.; Abbas, S.; Zhu, R.; Kwok, C.Y.T.; Heo, J.; Ju, S.; Wong, M.S. A Review of Dynamic Tree Behaviors: Measurement Methods on Tree Sway, Tree Tilt, and Root–Plate Movement. *Forests* **2021**, *12*, 379. [CrossRef]
2. James, K.R. Dynamic Loading of Trees. *J. Arboric.* **2003**, *29*, 165–171. [CrossRef]
3. Sagi, P.; Newson, T.; Miller, C.; Mitchell, S. Stem and Root System Response of a Norway Spruce Tree (*Picea abies* L.) under Static Loading. *Forestry* **2019**, *92*, 460–472. [CrossRef]
4. Schaetzl, R.J.; Burns, S.F.; Johnson, D.L.; Small, T.W. Tree Uprooting: Review of Impacts on Forest Ecology. *Vegetatio* **1988**, *79*, 165–176. [CrossRef]
5. Stephens, E.P. The Uprooting of Trees: A Forest Process. *Soil Sci. Soc. Am. J.* **1956**, *20*, 113–116. [CrossRef]
6. Hui, K.K.W.; Wong, M.S.; Kwok, C.Y.T.; Li, H.; Abbas, S.; Nichol, J.E. Unveiling Falling Urban Trees before and during Typhoon Higos (2020): Empirical Case Study of Potential Structural Failure Using Tilt Sensor. *Forests* **2022**, *13*, 359. [CrossRef]
7. Van Haaften, M.; Gardebroek, C.; Heijman, W.; Meuwissen, M.P.M. Injuries and Deaths Due to Tree Failure in The Netherlands: Analysis of Observational Data from 1998–2021. *Sci. Rep.* **2024**, *14*, 22415. [CrossRef]
8. Ylinen, A. *Über die Mechanische Schaftformtheorie der Bäume*; Silva Fennica; Technische Hochschule in Finnland: Helsinki, Finland, 1952; p. 50.
9. Tamate, S.; Kashiyama, T.; Sasanuma, T. A Trial of Pulling down Standing Trees. *J. Jpn. For. Res.* **1965**, *47*, 210–213. [CrossRef]
10. Fraser, A.I.; Gardiner, J.B.H. *Rooting and Stability in Sitka Spruce*; Bulletin; Forestry Commision: London, UK, 1967; p. 56.
11. Fraser, A.I. The Soil and Roots as Factors in Tree Stability. *Forestry* **1962**, *35*, 117–127. [CrossRef]
12. Sinn, G.; Wessolly, L. Zur sachgerechten Beurteilung der Stand-und Bruchsicherheit von Bäumen. *Neue Landsch.* **1988**, *33*.
13. Wessolly, L. Zwei neue zerstörungsfreie Messverfahren. *Gartenamt* **1989**, *34*, 587–591.
14. Wessolly, L.; Erb, M. *Handbuch der Baumstatik und Baumkontrolle*; Patzer Verlag: Berlin, Germany, 1998.
15. Krisans, O.; Caksa, L.; Matisons, R.; Rust, S.; Elferts, D.; Seipulis, A.; Jansons, A. A Static Pulling Test Is a Suitable Method for Comparison of the Loading Resistance of Silver Birch (*Betula pendula* Roth.) between Urban and Peri-Urban Forests. *Forests* **2022**, *13*, 127. [CrossRef]
16. Rust, S.; van Wassenaer, P. Tools for Tree Risk Assessment. In *Routledge Handbook of Urban Forestry*; Routledge: Abingdon, UK, 2017.
17. Lundström, T.; Stoffel, M.; Stöckli, V. Fresh-Stem Bending of Silver Fir and Norway Spruce. *Tree Physiol.* **2008**, *28*, 355–366. [CrossRef] [PubMed]
18. Neild, S.A.; Wood, C.J. Estimating Stem and Root-Anchorage Flexibility in Trees. *Tree Physiol.* **1999**, *19*, 141–151. [CrossRef]
19. Shah, D.U.; Reynolds, T.P.; Ramage, M.H. The Strength of Plants: Theory and Experimental Methods to Measure the Mechanical Properties of Stems. *J. Exp. Bot.* **2017**, *68*, 4497–4516. [CrossRef] [PubMed]
20. Stokes, A. Strain Distribution during Anchorage Failure of *Pinus pinaster* Ait. at Different Ages and Tree Growth Response to Wind-Induced Root Movement. *Plant Soil* **1999**, *217*, 17–27. [CrossRef]
21. Duperat, M.; Gardiner, B.; Ruel, J.-C. Wind and Snow Loading of Balsam Fir during a Canadian Winter: A Pioneer Study. *Forests* **2020**, *11*, 1089. [CrossRef]
22. Miyashita, A.; Suzuki, S. A Method for Measuring the Forces Acting on a Tree Trunk Using Strain Gauges. *PLoS ONE* **2021**, *16*, e0245631. [CrossRef]
23. Nickl, J.; Kolbe, S.; Schindler, D. Enhancing TreeMMoSys with a High-Precision Strain Gauge to Measure the Wind-Induced Response of Trees down to the Ground. *HardwareX* **2022**, *12*, e00379. [CrossRef]
24. James, K.R.; Kane, B. Precision Digital Instruments to Measure Dynamic Wind Loads on Trees during Storms. *Agric. For. Meteorol.* **2008**, *148*, 1055–1061. [CrossRef]
25. Angelou, N.; Gardiner, B.; Dellwik, E. Mean and Maximum Two Dimensional Wind Force on an Open-Grown Tree. *J. Wind. Eng. Ind. Aerodyn.* **2025**, *257*, 105966. [CrossRef]
26. Tippner, J.; Praus, L.; Brabec, M.; Sebera, V.; Vojackova, B.; Milch, J. Using 3D Digital Image Correlation in an Identification of Defects of Trees Subjected to Bending. *Urban For. Urban Green.* **2019**, *46*, 126513. [CrossRef]
27. Burcham, D.C.; Autio, W.R.; James, K.; Modarres-Sadeghi, Y.; Kane, B. Effect of Pruning Type and Severity on Vibration Properties and Mass of Senegal Mahogany (*Khaya senegalensis*) and Rain Tree (*Samanea saman*). *Trees* **2020**, *34*, 213–228. [CrossRef]
28. Sebera, V.; Praus, L.; Tippner, J.; Kunecký, J.; Čepela, J.; Wimmer, R. Using Optical Full-Field Measurement Based on Digital Image Correlation to Measure Strain on a Tree Subjected to Mechanical Load. *Trees* **2014**, *28*, 1173–1184. [CrossRef]
29. Hassinen, A.; Lemettinen, M.; Peltola, H.; Kellomäki, S.; Gardiner, B.A. A Prism-Based System for Monitoring the Swaying of Trees under Wind Loading. *Agric. For. Meteorol.* **1998**, *90*, 187–194. [CrossRef]
30. Angelou, N.; Dellwik, E.; Mann, J. Wind Load Estimation on an Open-Grown European Oak Tree. *Forestry* **2019**, *92*, 381–392. [CrossRef]
31. Detter, A.; Rust, S.; Krisans, O. Experimental Test of Non-Destructive Methods to Assess the Anchorage of Trees. *Forests* **2023**, *14*, 533. [CrossRef]

32. James, K.; Hallam, C.; Spencer, C. Measuring Tilt of Tree Structural Root Zones under Static and Wind Loading. *Agric. For. Meteorol.* **2013**, *168*, 160–167. [CrossRef]
33. Abbas, S.; Kwok, C.Y.T.; Hui, K.K.W.; Li, H.; Chin, D.C.W.; Ju, S.; Heo, J.; Wong, M.S. Tree Tilt Monitoring in Rural and Urban Landscapes of Hong Kong Using Smart Sensing Technology. *Trees For. People* **2020**, *2*, 100030. [CrossRef]
34. Chau, W.Y.; Wang, Y.-H.; Chiu, S.W.; Tan, P.S.; Leung, M.L.; Lui, H.L.; Wu, J.; Lau, Y.M.; Liu, K.-F.; Hau, B.C.H. Monitoring of Tree Tilt Motion Using Lorawan-Based Wireless Tree Sensing System (IoTT) during Super Typhoon Mangkhut. *Agric. For. Meteorol.* **2023**, *329*, 109282. [CrossRef]
35. Flesch, T.K.; Wilson, J.D. Wind and Remnant Tree Sway in Forest Cutblocks. II. Relating Measured Tree Sway to Wind Statistics. *Agric. For. Meteorol.* **1999**, *93*, 243–258. [CrossRef]
36. Göcke, L.; Rust, S.; Ruhl, F. Assessing the Anchorage and Critical Wind Speed of Urban Trees Using Root-Plate Inclination in High Winds. *Arboric. Urban For.* **2018**, *44*, 1–11. [CrossRef]
37. James, K.; Hallam, C.; Spencer, C. Tree Stability in Winds: Measurements of Root Plate Tilt. *Biosyst. Eng.* **2013**, *115*, 324–331. [CrossRef]
38. Kolbe, S.; Pfenning, M.; Schindler, D. Wind-Induced Torsional Vibration in a Ponderosa Pine Tree. *For. Ecol. Manag.* **2024**, *553*, 121638. [CrossRef]
39. Wu, Y.; Shao, Z. Measurement and Mechanical Analysis of the Strains–Stresses Induced by Tree-Pulling Experiments in Tree Stems. *Trees* **2016**, *30*, 675–684. [CrossRef]
40. Giachetti, A.; Zini, G.; Giambastiani, Y.; Bartoli, G. Field Measurements of Tree Dynamics with Accelerometers. *Forests* **2022**, *13*, 1243. [CrossRef]
41. Detter, A.; Rust, S.; Rust, C.; Risse, M. Determining Strength Limits for Standing Tree Stems from Bending Tests. In *Proceedings of the Conference and Abstracts Book of the European Conference of Arboriculture*; Giordano, L., Ferrini, F., Gonthier, P., Eds.; DISAFA Editions: Turin, Italy, 2014.
42. Spiegel, P.; Hintze, T.; Kopp, A.; Sahli, M.; Detter, A.; Queloz, V.; Prospero, S.; Heinzelmann, R. Synergistic Negative Effects of Ash Dieback and *Armillaria* Root Rot on Health and Stability of Mature Ash Trees. *For. Ecol. Manag.* **2025**, *580*, 122476. [CrossRef]
43. Sinn, G. Optische und Lasermessung der Standsicherheit von Bäumen. *Neue Landsch.* **1990**, *35*, 636–640.
44. Sinn, G.; Wessolly, L. A Contribution to the Proper Assessment of the Strength and Stability of Trees. *Arboric. J.* **1989**, *13*, 45–65. [CrossRef]
45. Lackmann, J.; Villwock, J. Statik starrer Körper. In *Dubbel*; Grote, K.-H., Feldhusen, J., Eds.; Springer: Berlin/Heidelberg, Germany, 2014; pp. 2–16.
46. Beléndez, T.; Neipp, C.; Beléndez, A. Large and Small Deflections of a Cantilever Beam. *Eur. J. Phys.* **2002**, *23*, 371–379. [CrossRef]
47. Bitiukov, D. Comparison of Theoretical Calculated Deflections According to the Euler-Bernoulli and Tymoshenko Beam Models with Experimentally Obtained. *Build. Constr. Theory Pract.* **2025**, 100–109. [CrossRef]
48. Bourbaki, N. Elements of Mathematics. In *2: [6.] Integration*; Springer: Berlin/Heidelberg, Germany, 2004; ISBN 978-3-540-20585-2.
49. Cannell, M.G.R.; Morgan, J. Young's Modulus of Sections of Living Branches and Tree Trunks. *Tree Physiol.* **1987**, *3*, 355–364. [CrossRef] [PubMed]
50. Greiner, W. Theoretische Physik: Ein Lehr- und Übungsbuch. In *1: Mechanik I*; Deutsch: Frankfurt am Main, Germany, 1984; ISBN 3-87144-800-1.
51. Greiner, W. Theoretische Physik: Ein Lehr- und Übungsbuch. In *1: Mechanik II*; Deutsch: Frankfurt am Main, Germany, 1989; ISBN 3-87144-700-5.
52. Maki, A.; Kuenzi, E. *Deflection and Stresses of Tapered Wood Beams*; U.S. Forest Service Research Paper; USDA FPL: Madison, WI, USA, 1965; p. 56.
53. Gerthsen, C.; Kneser, H.O.; Vogel, H. *Gerthsen Kneser Vogel Physik*; Springer: Berlin/Heidelberg, Germany, 1982; ISBN 3-540-07876-2.
54. Morgan, J.; Cannell, M.G.R. Structural Analysis of Tree Trunks and Branches: Tapered Cantilever Beams Subject to Large Deflections under Complex Loading. *Tree Physiol.* **1987**, *3*, 365–374. [CrossRef] [PubMed]
55. Murata, K.; Kanazawa, T. Determination of Young's Modulus and Shear Modulus by Means of Deflection Curves for Wood Beams Obtained in Static Bending Tests. *Holzforschung* **2007**, *61*, 589–594. [CrossRef]
56. Orear, J. *Physics*; Macmillan: New York, NY, USA, 1979.
57. Spiegel, M.R. *Schaum's Outline of Theory and Problems of Theoretical Mechanics: With an Introduction to Lagrange's Equations and Hamiltonian Theory*; Schaum's Outline Series; McGraw-Hill: New York, NY, USA, 1980; ISBN 978-0-07-084357-8.
58. R Core Team. *R: A Language and Environment for Statistical Computing*; R Foundation for Statistical Computing: Vienna, Austria, 2025.
59. Buza, Á.K.; Divós, F. Root Stability Evaluation with Non-Destructive Techniques. *Acta Silv. Lignaria Hung.* **2016**, *12*, 125–134. [CrossRef]
60. Antony, F.; Jordan, L.; Schimleck, L.R.; Clark, A.; Souter, R.A.; Daniels, R.F. Regional Variation in Wood Modulus of Elasticity (Stiffness) and Modulus of Rupture (Strength) of Planted Loblolly Pine in the United States. *Can. J. For. Res.* **2011**, *41*, 1522–1533. [CrossRef]

61. Hoffmeyer, D.; Damanpack, A.R. Bending and Torsion Induced Stresses in Cylindrically Orthotropic and Inhomogeneous Timber Beams. *Finite Elem. Anal. Des.* **2024**, *229*, 104072. [CrossRef]
62. de Langre, E. Effects of Wind on Plants. *Annu. Rev. Fluid Mech.* **2008**, *40*, 141–168. [CrossRef]
63. Jackson, T.D.; Sethi, S.; Dellwik, E.; Angelou, N.; Bunce, A.; Van Emmerik, T.; Duperat, M.; Ruel, J.-C.; Wellpott, A.; Van Bloem, S.; et al. The Motion of Trees in the Wind: A Data Synthesis. *Biogeosciences* **2021**, *18*, 4059–4072. [CrossRef]